Design of minimum-order allpass-based IIR multi-notch filters

Ivan Krstić[a,*], Mina Vasković Jovanović[a]

[a]*Faculty of Engineering, University of Kragujevac, 34000 Kragujevac, Serbia*

Abstract

The paper investigates the design methods for the minimum-order allpass-based infinite impulse response multi-notch filters. Monotonically decreasing nature of the stable allpass filter's phase response allows the formulation of the magnitude response specifications of the allpass-based multi-notch filter as the linear equality and inequality constraints in unknown allpass filter coefficients. As not all allpass filters satisfying mentioned constraints are of the same practical interest, several design methods minimizing various cost functions are proposed. One of these methods outperforms existing design methods in terms of stability margin, while utilization of other methods can result in higher area under the passbands squared magnitude response. Proposed methods are also compared with some of the existing infinite impulse response multi-notch filter design methods, whose lower complexity counterparts are derived by means of conclusions drawn and notations introduced while deriving the proposed design methods.

Keywords: digital multi-notch filter, allpass filter, magnitude response, linear and quadratic programming

1. Introduction

In wide range of practical applications, from physiological signals preprocessing [1, 2, 3] to satellite system receivers [4], exist necessity for the multi-notch

*Corresponding author

Email addresses: ivan.krstic@kg.ac.rs (Ivan Krstić), mina.vaskovic.jovanovic@kg.ac.rs (Mina Vasković Jovanović)

filters whose role is to eliminate certain frequency components from the input signal's spectrum, while keeping the other components intact. Frequency response of these filters in ideal case is of the following form

$$H_d\left(e^{j\omega}\right) = \begin{cases} 0, & \omega \in \{\omega_{n,k} \,|\, k = 1,\, 2,\, \ldots,\, K\} \\ 1, & \text{otherwise} \end{cases}, \tag{1}$$

where $\omega_{n,k}$ denotes frequency of the k-th input signal's spectral component that needs to be suppressed, while K denotes total number of such frequencies. Previous equation suggests zero notch-bandwidths which cannot be practically realized, and would also be highly undesirable having in mind that transient response duration to the sinusoidal interferences of frequencies $\omega_{n,k}$, for $k = 1,\, 2,\, \ldots,\, K$, in case of zero notch-bandwidths, is infinitely long [5, 6, 7]. Therefore, specifications of practical multi-notch filter also comprise non-zero notch-bandwidths $\Delta\omega_k$, $k = 1,\, 2,\, \ldots,\, K$, defining the left- and right-hand cutoff frequencies

$$\begin{aligned} \omega_{l,k} &= \omega_{n,k} - \Delta\omega_k/2, \\ \omega_{r,k} &= \omega_{n,k} + \Delta\omega_k/2, \end{aligned} \tag{2}$$

at which attenuation in dB should be less than or equal to a. It should be noted that higher the $\Delta\omega_k$ is (therefore lower radius of the pole whose angle is closest to the $\omega_{n,k}$), transient response duration to sinusoidal interference of frequency $\omega_{n,k}$ is shorter [5, 6, 7]. Attenuation at which notch-bandwidths are specified, a, usually equals 3 dB.

Generally, digital multi-notch filters can be designed either as infinite impulse response (IIR) or finite impulse response filters. Aside the fact that linear passbands phase response can be easily obtained by finite impulse response structure which is inherently stable, obtained multi-notch filter order is significantly higher compared to IIR filter counterpart. Although the design methods for the higher order IIR multi-notch filters, characterized by improved magnitude and/or phase response, are also considered in the literature [8, 9, 10, 11, 12], a design methods for the minimum-order (ie. the order equals double the number of notch frequencies) IIR multi-notch filters are considered in this paper. The

majority of the minimum-order IIR multi-notch filter design methods belong to one of the four approaches briefly discussed bellow, where only methods whose utilization result in the exact satisfaction of the notch frequencies specifications are considered.

Conventional approach to the IIR multi-notch filter design is to cascade several IIR notch filters [13, 14]. This approach is applicable if number of notch frequencies is small and notch-bandwidths are narrow, otherwise, magnitude response of obtained filters exhibits uncontrollable passbands gain between notch frequencies [15, 16].

Optimum poles placement-based design methods [17, 18, 19, 20] formulate the IIR multi-notch filter design problem as the minimization problem in unknown poles' locations, as zeros are located at the unit circle at phase angles equal to the specified notch frequencies. While method [17] suboptimally determines the unknown poles using iterative Steiglitz-McBride scheme [21] and quadratic programming, methods presented in [18, 20] determine the poles' angles using metaheuristic algorithms assuming known pole radii determined directly from the corresponding 3 dB notch-bandwidths. The main drawback of the optimum poles placement methods, apart from the facts that method [17] does not consider notch-bandwidths' specifications, while methods [18, 20] are applicable only if attenuation at cutoff frequencies equals 3 dB, is that extremal values of the magnitude response are not necessarily equal in all passbands.

Methods of the squared magnitude function approach [22, 23] are based on the design of the denominator of the IIR multi-notch filter squared magnitude response. Namely, mentioned denominator is first expressed as a rational polynomial function of $x = \tan^2(\omega/2) = -\left[(z-1)/(z+1)\right]^2_{z=e^{j\omega}}$ in [22] and a polynomial of $x = \cos(\omega) = 0.5\left(z+z^{-1}\right)_{z=e^{j\omega}}$ in [23], and then designed by the local maxima positions of the magnitude response and an additional parameter by which value realized notch-bandwidths are guaranteed to be less than the specified ones.

Finally, allpass-based design methods [24, 25, 16, 26, 27] start from the IIR multi-notch filter transfer function expressed as $H(z) = \frac{1}{2}(1 + A(z))$, where

$A(z)$ is the transfer function of the stable allpass filter of order $2K$. It is well known that such transfer functions can be realized using efficient lattice structures [13, 16]. As phase response of the stable allpass filter is monotonically decreasing function in frequency, IIR multi-notch filter's magnitude response specifications can be transformed into corresponding allpass filter's phase response specifications that can be expressed in linear form. Method in [26] assumes the identical pole radii of all poles and unknown coefficients are determined such that specifications of notch frequencies positions are satisfied. On the other hand, methods presented in [25, 24, 16] utilize notch and left-hand cutoff frequencies or notch and right-hand cutoff frequencies as filter design constraints, while method presented in [27] utilizes notch and both left- and right-hand cutoff frequencies. All of mentioned allpass-based IIR multi-notch design methods are non-iterative and although methods from [16, 26, 24, 25] consider attenuation value at the cutoff frequencies equal to 3 dB, some of them, that is methods presented in [24, 25, 16], can be generalized to a case of an arbitrary attenuation value at which notch-bandwidths are specified. It should be noted that transfer functions obtained by utilization of methods [22, 23] can be also expressed as $H(z) = \frac{1}{2}(1 + A(z))$, however, these methods are not considered to be allpass-based in this paper, as specifications of the magnitude response are not transformed into phase response specifications of the corresponding allpass filter.

To the best of our knowledge, utilization of the existing minimum-order IIR multi-notch filter design methods, except the ones presented in [22, 23], in general, does not result in satisfaction of specifications regarding the maximum attenuation value in passbands, which is followed by distortion of the input signal's spectrum components. Furthermore, there is no design method that minimizes the maximum poles radius, thus maximizing the filter's stability margin. In this paper, a new minimum-order allpass-based IIR multi-notch filter design problem setting is first introduced and several design methods minimizing various cost functions are proposed. One of these methods outperforms existing methods in terms of stability margin, while utilization of other methods

can result in higher area under the passbands squared magnitude response.

The rest of the paper is organized as follows. Allpass-based IIR multi-notch filter design problem is formulated in Sec. 2, while several design methods are discussed in Sec. 3. Filters obtained using the proposed methods are compared to filters obtained using existing design methods in Sec. 4. Finally, concluding remarks are drawn in Sec. 5.

2. Problem Formulation

As already mentioned, specifications of the IIR multi-notch filter magnitude response comprise notch frequencies positions and notch-bandwidths defining left- and right-hand cutoff frequencies, Eq. (2), specified at attenuation value of a in dB. In other words, following should be satisfied

$$H\left(e^{j\omega_{n,k}}\right) = 0, \quad k = 1, 2, \ldots, K, \tag{3}$$

$$-20\log_{10}\left|H\left(e^{j\omega}\right)\right| \leq a, \quad \omega \in \mathcal{P}, \tag{4}$$

where $\mathcal{P}$ denotes set of frequencies in the passbands

$$\mathcal{P} = (0, \pi) \setminus \bigcup_{k=1}^{K} \left\{\omega \,|\, \omega_{l,k} < \omega < \omega_{r,k}\right\}. \tag{5}$$

Transfer function of the allpass-based minimum-order IIR multi-notch filter is of the following form

$$H(z) = \frac{1}{2}\left(1 + A(z)\right), \tag{6}$$

where $A(z)$ is the transfer function of the stable allpass filter of order $2K$,

$$A(z) = z^{-2K} P\left(z^{-1}\right) P^{-1}(z), \tag{7}$$

and

$$P(z) = 1 + \sum_{i=1}^{2K} p_i z^{-i}, \tag{8}$$

while $p_1, p_2, \ldots, p_{2K}$ are the allpass filter coefficients. Substituting $z = e^{j\omega}$ in Eq. (6), followed by simple algebraic calculation, the frequency response of the allpass-based IIR multi-notch filter can be expressed as

$$H\left(e^{j\omega}\right) = e^{j\frac{\varphi(\omega)}{2}} \cos\frac{\varphi(\omega)}{2}, \tag{9}$$

where $\varphi(\omega)$ is the phase response of the allpass filter $A(z)$,

$$\varphi(\omega) = -2K\omega - 2\arg\left\{P\left(e^{j\omega}\right)\right\}. \tag{10}$$

Employing the fact that the phase response $\varphi(\omega)$ of the stable allpass filter $A(z)$ is monotonically decreasing function for $\omega \in (0, \pi)$, while $\varphi(0) = 0$ and $\varphi(\pi) = -2K\pi$ [13, 24], from Eq. (9) it can be concluded that the magnitude response specifications given by Eqs. (3) and (4) are equivalent to

$$\cos\frac{\varphi(\omega_{n,k})}{2} = 0, \tag{11}$$

$$(-1)^{k-1}\cos\frac{\varphi(\omega_{l,k})}{2} \geq 10^{-a/20}, \tag{12}$$

$$(-1)^{k}\cos\frac{\varphi(\omega_{r,k})}{2} \geq 10^{-a/20}, \tag{13}$$

for $k = 1, 2, \ldots, K$.

Now, by means of trigonometrical identities

$$\cos(\arg\{\cdot\}) = \frac{\mathrm{Re}\{\cdot\}}{|\cdot|}, \quad \sin(\arg\{\cdot\}) = \frac{\mathrm{Im}\{\cdot\}}{|\cdot|},$$

and Eq. (10), cosine and sine of the half allpass filter's phase response can be rewritten in terms of its coefficients as

$$\cos\frac{\varphi(\omega)}{2} = \frac{R(\omega)}{\sqrt{R^2(\omega) + Q^2(\omega)}}, \tag{14}$$

$$\sin\frac{\varphi(\omega)}{2} = \frac{Q(\omega)}{\sqrt{R^2(\omega) + Q^2(\omega)}}, \tag{15}$$

where

$$R(\omega) = p_K + (1 + p_{2K})\cos(K\omega) + \sum_{i=1}^{K-1}(p_{K+i} + p_{K-i})\cos(i\omega), \tag{16}$$

$$Q(\omega) = (p_{2K} - 1)\sin(K\omega) + \sum_{i=1}^{K-1}(p_{K+i} - p_{K-i})\sin(i\omega). \tag{17}$$

Utilizing Eq. (14) and observing that

$$\begin{aligned}(-1)^{k} Q(\omega_{l,k}) &\geq 0,\\ (-1)^{k} Q(\omega_{r,k}) &\geq 0,\end{aligned} \tag{18}$$

which follows from the monotonically decreasing nature of $\varphi(\omega)$ and Eq. (15), Eqs. (11), (12) and (13), after some algebraic manipulations, can be rewritten as

$$R(\omega_{n,k}) = 0, \tag{19}$$

$$(-1)^{k-1}\left[\sin\alpha \cdot R(\omega_{l,k}) + \cos\alpha \cdot Q(\omega_{l,k})\right] \geq 0, \tag{20}$$

$$(-1)^{k}\left[\sin\alpha \cdot R(\omega_{r,k}) - \cos\alpha \cdot Q(\omega_{r,k})\right] \geq 0, \tag{21}$$

for $k = 1, 2, \ldots, K$, respectively, where

$$\cos\alpha = 10^{-\alpha/20} \tag{22}$$

and $0 < \alpha < \pi/2$.

Having in mind previous discussion, design problem of the minimum-order allpass-based IIR multi-notch filter reduces to determination of unknown coefficients of the corresponding stable allpass filter such that Eqs. (19), (20) and (21) are satisfied. However, not all allpass filter coefficients satisfying mentioned equations are of the same interest since the increase in values of the left-hand sides of Eqs. (20) and (21) reflects the decrease of the attenuation at the corresponding cutoff frequencies, which is a consequence of the fact that these equations are derived from Eq. (4) by considering the monotonically decreasing nature of the stable allpass filter's phase response. This, on the other hand, is usually followed by increase of the corresponding pole radius, ie. the prolonged duration of the transient response to the sinusoidal interference. Furthermore, filters having lower maximum pole radius have higher stability margin [28, 23]. Therefore, values of the left-hand sides of Eqs. (20) and (21) should be treated with great concern.

3. Proposed Design Methods

By closely observing Eq. (19), defining a system of K linear equations in $2K$ unknown allpass filter coefficients, it can be concluded that it can be rewritten

as a square system of linear equations in K unknowns

$$u_i = \begin{cases} p_K / (1 + p_{2K}), & i = 1 \\ (p_{K+i-1} + p_{K-i+1}) / (1 + p_{2K}), & 2 \le i \le K \end{cases}, \tag{23}$$

as

$$\mathbf{\Phi}_N \cdot \mathbf{u} = \boldsymbol{\gamma}_N, \tag{24}$$

where $\mathbf{u} = [u_i]$ is the $K \times 1$ vector, while $\mathbf{\Phi}_N = \left[\phi_{ki}^{(N)}\right]$ and $\boldsymbol{\gamma}_N = \left[\gamma_k^{(N)}\right]$ are $K \times K$ square matrix and $K \times 1$ vector, respectively, with elements

$$\begin{aligned} \phi_{ki}^{(N)} &= \cos\left((i-1)\,\omega_{n,k}\right), \\ \gamma_k^{(N)} &= -\cos\left(K\omega_{n,k}\right). \end{aligned} \tag{25}$$

Incorporating specifications regarding the notch frequencies positions given by $\mathbf{u} = \mathbf{\Phi}_N^{-1} \cdot \boldsymbol{\gamma}_N$, note Eq. (24), in Eqs. (20) and (21), it follows that stable allpass-based IIR multi-notch filter complies with magnitude response specifications if

$$\mathbf{\Phi}_L \cdot \mathbf{v} - \boldsymbol{\gamma}_L \ge 0, \tag{26}$$

$$\mathbf{\Phi}_R \cdot \mathbf{v} - \boldsymbol{\gamma}_R \ge 0, \tag{27}$$

where $\mathbf{v} = [v_i]$ is the $K \times 1$ vector with elements

$$v_i = \begin{cases} (1 + p_{2K}) / (1 - p_{2K}), & i = 1 \\ (p_{K-i+1} - p_{K+i-1}) / (1 - p_{2K}), & 2 \le i \le K \end{cases}, \tag{28}$$

while $\mathbf{\Phi}_L = \left[\phi_{ki}^{(L)}\right]$ and $\mathbf{\Phi}_R = \left[\phi_{ki}^{(R)}\right]$ are $K \times K$ matrices, $\boldsymbol{\gamma}_L = \left[\gamma_k^{(L)}\right]$ and $\boldsymbol{\gamma}_R = \left[\gamma_k^{(R)}\right]$ are $K \times 1$ vectors, with elements

$$\begin{aligned} \phi_{ki}^{(L)} &= \begin{cases} (-1)^{k-1} \sin\alpha \cdot \left[\cos\left(K\omega_{l,k}\right) + \mathbf{c}\left(\omega_{l,k}\right) \cdot \mathbf{u}\right], & i = 1 \\ (-1)^{k} \cos\alpha \cdot \sin\left((i-1)\,\omega_{l,k}\right), & 2 \le i \le K \end{cases}, \\ \phi_{ki}^{(R)} &= \begin{cases} (-1)^{k} \sin\alpha \cdot \left[\cos\left(K\omega_{r,k}\right) + \mathbf{c}\left(\omega_{r,k}\right) \cdot \mathbf{u}\right], & i = 1 \\ (-1)^{k} \cos\alpha \cdot \sin\left((i-1)\,\omega_{r,k}\right), & 2 \le i \le K \end{cases}, \\ \gamma_k^{(L)} &= (-1)^{k-1} \cos\alpha \cdot \sin\left(K\omega_{l,k}\right), \\ \gamma_k^{(R)} &= (-1)^{k-1} \cos\alpha \cdot \sin\left(K\omega_{r,k}\right), \end{aligned} \tag{29}$$

where $\mathbf{c}(\omega)$ denotes vector

$$\mathbf{c}(\omega) = [1 \quad \cos\omega \quad \cos(2\omega) \quad \ldots \quad \cos((K-1)\omega)]. \tag{30}$$

As Eq. (18) and $0 \leq p_{2K} < 1$ are used while deriving Eq. (26), they have to be included as design constraints to ensure stability of the allpass-based IIR multi-notch filter. Utilizing Eqs. (28) and (29), these additional constraints can be formulated as linear inequalities

$$\begin{bmatrix} -1 & \mathbf{0}_{1\times(K-1)} \\ \mathbf{0}_{K\times 1} & \widetilde{\mathbf{\Phi}}_L \\ \mathbf{0}_{K\times 1} & \widetilde{\mathbf{\Phi}}_R \end{bmatrix} \mathbf{v} \leq \begin{bmatrix} -2 \\ \boldsymbol{\gamma}_L \\ \boldsymbol{\gamma}_R \end{bmatrix}, \tag{31}$$

where $\mathbf{\Phi}_L$ and $\mathbf{\Phi}_R$ are partitioned as

$$\begin{aligned} \mathbf{\Phi}_L &= \begin{bmatrix} \boldsymbol{\eta}_L & \widetilde{\mathbf{\Phi}}_L \end{bmatrix}, \\ \mathbf{\Phi}_R &= \begin{bmatrix} \boldsymbol{\eta}_R & \widetilde{\mathbf{\Phi}}_R \end{bmatrix}, \end{aligned} \tag{32}$$

while $\boldsymbol{\eta}_L$ and $\boldsymbol{\eta}_R$ are column vectors.

Therefore, allpass-based IIR multi-notch filter design problem reduces to determination of vector $\mathbf{v}$ such that some objective function is optimized subject to constrains given by Eqs. (26), (27) and (31). Once vector $\mathbf{v}$ is determined, unknown allpass filter coefficients can be determined from Eqs. (23) and (28) as

$$p_i = \begin{cases} (v_1 u_{K-i+1} + v_{K-i+1}) / (v_1 + 1), & 1 \leq i \leq K-1 \\ 2v_1 u_1 / (v_1 + 1), & i = K \\ (v_1 u_{i-K+1} - v_{i-K+1}) / (v_1 + 1), & K+1 \leq i \leq 2K-1 \\ (v_1 - 1) / (v_1 + 1), & i = 2K \end{cases}. \tag{33}$$

The first proposed design method, referred to as *Method A*, minimizes the geometric mean of the multi-notch filter pole radii, $\sqrt[4]{p_{2K}}$, subject to constraints given by Eqs. (26), (27) and (31). Since from Eq. (28) it follows that

$$\frac{\mathrm{d}v_1}{\mathrm{d}p_{2K}} > 0,$$

minimization of the geometric mean of IIR multi-notch filter pole radii reduces to minimization of v_1. Therefore, a linear programming minimization problem

characterizing the proposed *Method A* reads

$$\begin{array}{ll} \underset{\mathbf{v}}{\text{minimize}} & v_1 \\ \text{subject to:} & \text{Eqs. (26), (27), (31)} \end{array} . \tag{34}$$

The second proposed design method, referred to as *Method B*, minimizes the maximum of the left-hand sides of Eqs. (26) and (27) subject to constraints given by Eqs. (26), (27) and (31). Therefore, *Method B* is characterized by the following linear programming minimization problem

$$\begin{array}{ll} \underset{\mathbf{v},\,\delta}{\text{minimize}} & \delta \\ \text{subject to:} & \text{Eqs. (26), (27) and (31)}, \\ & \left[\begin{array}{c} \boldsymbol{\Phi}_L \\ \boldsymbol{\Phi}_R \end{array} \right] \mathbf{v} - \left[\begin{array}{c} \boldsymbol{\gamma}_L \\ \boldsymbol{\gamma}_R \end{array} \right] \leq \delta \cdot \mathbf{1}_{2K\times 1} \end{array} . \tag{35}$$

The third proposed design method, referred to as *Method C*, minimizes the weighted Euclidean norm of the left-hand sides of Eqs. (26) and (27),

$$\left(\boldsymbol{\Phi}_L \cdot \mathbf{v} - \boldsymbol{\gamma}_L\right)^{\mathrm{T}} \mathbf{W}_L^{\mathrm{T}} \mathbf{W}_L \left(\boldsymbol{\Phi}_L \cdot \mathbf{v} - \boldsymbol{\gamma}_L\right) + \left(\boldsymbol{\Phi}_R \cdot \mathbf{v} - \boldsymbol{\gamma}_R\right)^{\mathrm{T}} \mathbf{W}_R^{\mathrm{T}} \mathbf{W}_R \left(\boldsymbol{\Phi}_R \cdot \mathbf{v} - \boldsymbol{\gamma}_R\right),$$

subject to constraints given by Eqs. (26), (27) and (31), where $\mathbf{W}_L$ and $\mathbf{W}_R$ are $K \times K$ diagonal matrices with nonnegative elements $w_k^{(L)} \in [0,\, 1]$ and $w_k^{(R)} \in [0, 1\,]$ on their diagonals, respectively, while the superscript T denotes the transpose matrix operator. Therefore, *Method C* is characterized by the following quadratic programming minimization problem

$$\begin{array}{ll} \underset{\mathbf{v}}{\text{minimize}} & \mathbf{v}^{\mathrm{T}} \left(\boldsymbol{\Phi}_L^{\mathrm{T}} \mathbf{W}_L^{\mathrm{T}} \mathbf{W}_L \boldsymbol{\Phi}_L + \boldsymbol{\Phi}_R^{\mathrm{T}} \mathbf{W}_R^{\mathrm{T}} \mathbf{W}_R \boldsymbol{\Phi}_R \right) \mathbf{v} \\ & \quad -2 \left(\boldsymbol{\gamma}_L^{\mathrm{T}} \mathbf{W}_L \boldsymbol{\Phi}_L + \boldsymbol{\gamma}_R^{\mathrm{T}} \mathbf{W}_R \boldsymbol{\Phi}_R \right) \mathbf{v} \\ \text{subject to:} & \text{Eqs. (26), (27) and (31)} \end{array} . \tag{36}$$

Selection of weighting factors $w_k^{(L)}$ and $w_k^{(R)}$, $k = 1,\, 2,\, \ldots,\, K$, can be based on either some heuristics or some optimality criteria. In this paper, three heuristic options to select weighting factors are proposed:

1. $\mathbf{W}_L = \mathrm{I}$, $\mathbf{W}_R = \mathbf{0}$, where I denotes the identity matrix. In other words, Euclidean norm of the left-hand side of Eq. (26) is minimized subject to

constraints given by Eqs. (26), (27) and (31). If weighting factors are selected this way, *Method C* is referred to as *Method C-L*.

2. $\mathbf{W}_L = \mathbf{0}$, $\mathbf{W}_R = \mathrm{I}$. In this case, Euclidean norm of the left-hand side of Eq. (27) is minimized subject to constraints given by Eqs. (26), (27) and (31). If weighting factors are selected this way, *Method C* is referred to as *Method C-R*.
3. $\mathbf{W}_L = \mathbf{W}_R = \mathrm{I}$, ie. Euclidean norm of left-hand sides of both Eqs. (26) and (27) is minimized subject to constraints given by Eqs. (26), (27) and (31). If weighting factors are selected this way, *Method C* is referred to as *Method C-LR*.

As stated before, the selection of weighting factors can also be performed to comply with a given optimality criteria subject to compliance with Eqs. (26), (27) and (31). When minimization of the maxium radius of the IIR multi-notch filter poles, denoted by $\rho_{\max}$, is considered, weighting factors are determined such that

$$[\mathbf{W}_L^* \quad \mathbf{W}_R^*] = \underset{\mathbf{W}_L,\, \mathbf{W}_R}{\arg\min} \ \rho_{\max}\left(\mathbf{W}_L,\, \mathbf{W}_R\right). \tag{37}$$

In the paper, optimization problem given by previous equation is solved using Particle Swarm Optimization (PSO) algorithm. If weighting factors are determined in this manner, *Method C* is referred to as *Method C-M*.

4. Comparison with the Existing Design Methods

Proposed design methods are only compared to existing design methods that guarantee the satisfaction of notch frequencies positions' specifications, and either consider the arbitrary attenuation value at which cutoff frequencies are specified, or can be generalized to such a case. Examination of the existing literature shows that there are only four such methods: two of which are from [24, 25, 16], the third one is proposed in [23], while the fourth one is from [27]. Furthermore, transfer functions obtained using these existing design methods can be alternatively derived using conclusions drawn and notations introduced in the previous sections as follows:

1) *Method I* from [16] utilizes notch and left-hand cutoff frequencies' specifications in the design process, while the attenuation at left-hand cutoff frequencies equals 3 dB. It should be noted that *Method I* from [16] is practically the same as the methods presented in [24, 25] with overcame limitations regarding to tangent operations. Generalization of this method, in the following text referred to as *Method D*, to handle arbitrary attenuation value at which cutoff frequencies are specified, is equivalent to equating the left-hand side of Eq. (26) to zero, ie. $\mathbf{v}$ can be determined as

$$\mathbf{v} = \mathbf{\Phi}_L^{-1} \cdot \boldsymbol{\gamma}_L. \tag{38}$$

IIR multi-notch filters designed by *Method D* do not necessarily satisfy magnitude response specifications regarding the maximum attenuation in passbands since Eq. (27) is not utilized by the design method. Furthermore, as vector $\mathbf{v}$, given by Eq. (38), is also a solution to the unconstrained optimization problem with Euclidean norm of the left-hand sides of Eq. (26) as objective function, if Eq. (27) is satisfied by filter obtained using *Method D*, the same filter is also obtained by *Method C-L*.

2) *Method II* from [16] utilizes notch and right-hand cutoff frequencies' specifications in the design process, while the attenuation at right-hand cutoff frequencies equals 3 dB. From Eq. (27), it follows that vector $\mathbf{v}$, that corresponds to generalization of *Method II* [16], in the following text referred to as *Method E*, to handle arbitrary attenuation value at which cutoff frequencies are specified, can be determined as

$$\mathbf{v} = \mathbf{\Phi}_R^{-1} \cdot \boldsymbol{\gamma}_R. \tag{39}$$

Since Eq. (26) is not utilized by this design method, IIR multi-notch filters designed using *Method E* do not necessarily satisfy magnitude response specifications regarding the maximum attenuation value in passbands. As vector $\mathbf{v}$, given by Eq. (39), is also a solution to the unconstrained optimization problem with Euclidean norm of the left-hand sides of Eq. (27) as objective function, if Eq. (26) is satisfied by filter obtained using *Method E*, the same

filter is also obtained by *Method C-R*.

3) Method in [23] utilizes the fact that for any set of frequencies, $\{\widetilde{\omega}_k \,|\, \omega_{r,k} < \widetilde{\omega}_k < \omega_{l,k+1},\, 1 \leq k \leq K-1\}$, where local maxima of the magnitude response occur, unknown coefficients can be determined such that magnitude response specifications are satisfied, if geometric mean of multi-notch filter pole radii is greater than some value. Although the method proposed in [23] starts from the denominator expressed as a positive polynomial of $x = \cos(\omega)$ which is designed by a shape factor (which is uniquely determined by the geometric mean of the pole radii) and the local maxima positions of the magnitude response, the computationally less intensive approach to the design of the same transfer functions as are those obtained by [23] is discussed in the following text. Discussed approach is referred to as *Method F*.

Since at frequencies where local maxima of the magnitude response occur one has that

$$\sin \frac{\varphi(\widetilde{\omega}_k)}{2} = 0, \tag{40}$$

for $k = 1, 2, \ldots, K-1$, from Eq. (15) it follows that

$$Q(\widetilde{\omega}_k) = 0, \tag{41}$$

for $k = 1, 2, \ldots, K-1$, which in matrix notation reads

$$\widetilde{\mathbf{\Phi}} \cdot \widetilde{\mathbf{v}} = \widetilde{\boldsymbol{\gamma}}, \tag{42}$$

where $\mathbf{v}$ is partitioned as

$$\mathbf{v} = \begin{bmatrix} v_1 \\ \widetilde{\mathbf{v}} \end{bmatrix}, \tag{43}$$

while $\widetilde{\mathbf{\Phi}} = \left[\widetilde{\phi}_{ki}\right]$ and $\widetilde{\boldsymbol{\gamma}} = [\widetilde{\gamma}_k]$ are $(K-1) \times (K-1)$ matrix and $(K-1) \times 1$ column vector, respectively, with elements

$$\begin{aligned} \widetilde{\phi}_{ki} &= \sin(i\widetilde{\omega}_k), \\ \widetilde{\gamma}_k &= -\sin(K\widetilde{\omega}_k). \end{aligned} \tag{44}$$

Therefore, vector $\widetilde{\mathbf{v}}$ can be determined from Eq. (42) as $\widetilde{\mathbf{v}} = \widetilde{\mathbf{\Phi}}^{-1} \cdot \widetilde{\boldsymbol{\gamma}}$. On the other hand, v_1, if not given (which is the case when the maximization of the area under the passbands squared magnitude response is considered in [23]), is determined such that geometric mean of multi-notch filter pole radii is minimized for a given set of frequencies where local maxima of the magnitude response occur,

$$v_1 = \max_k \ \lambda_k, \tag{45}$$

where

$$[\lambda_k]_{2K\times 1} = \begin{bmatrix} \boldsymbol{\gamma}_L - \widetilde{\mathbf{\Phi}}_L \cdot \widetilde{\mathbf{v}} \\ \boldsymbol{\gamma}_R - \widetilde{\mathbf{\Phi}}_R \cdot \widetilde{\mathbf{v}} \end{bmatrix} \oslash \begin{bmatrix} \boldsymbol{\eta}_L \\ \boldsymbol{\eta}_R \end{bmatrix}, \tag{46}$$

which follows from Eqs. (26), (27) and (32), and operator $\oslash$ is the Hadamard division matrix operator.

Three heuristic options and two optimality criteria for selection of frequencies $\widetilde{\omega}_k$, $1 \leq k \leq K-1$, are proposed in [23]. Heuristic options are:

(a) Projection of averaged notch frequencies (PANF):

$$\widetilde{\omega}_k = \frac{\omega_{n,k} + \omega_{n,k+1}}{2}.$$

For this selection, *Method F* is referred to as *Method F-PANF*.

(b) Average of projected notch frequencies (APNF):

$$\widetilde{\omega}_k = \arccos \frac{\cos \omega_{n,k} + \cos \omega_{n,k+1}}{2}.$$

In this case, *Method F* is referred to as *Method F-APNF*.

(c) Local maxima positions (LMPN) of $N(\omega) = \prod_{i=1}^{K} (\cos\omega - \cos\omega_{n,i})^2$, ie.

$$\widetilde{\omega}_k \mid N'(\omega) = 0 \ .$$

In this case, *Method F* is referred to as *Method F-LMPN*.

On the other hand, optimality criteria considered in [23] are the minimization of geometric mean of multi-notch filter pole radii and the maximization of the area under the passbands squared magnitude response for a given value

of the geometric mean of the pole radii. The solutions when these optimality criteria considered are obtained using the PSO algorithm in [23].

Note that proposed *Method A* also minimizes the geometric mean of the pole radii, while at the same time its computational complexity is considerably lower compared to the existing design method in [23].

Furthermore, as the area under the passbands squared magnitude response

$$A_p = \int\limits_{\omega\in\mathcal{P}} \left|H\left(e^{j\omega}\right)\right|^2 \mathrm{d}\omega, \tag{47}$$

by means of Eqs. (9) and (15) can be expressed as

$$A_p = \int\limits_{\omega\in\mathcal{P}} \cos^2\frac{\varphi\left(\omega\right)}{2}\mathrm{d}\omega = \int\limits_{\omega\in\mathcal{P}} \left[1 - \frac{Q^2\left(\omega\right)}{R^2\left(\omega\right)+Q^2\left(\omega\right)}\right]\mathrm{d}\omega, \tag{48}$$

maximization of A_p subject to constraints given by Eqs. (26), (27) and (31), and specified value of the geometric mean of the pole radii, reduces to the following minimization problem

$$\begin{array}{ll} \underset{\widetilde{\mathbf{v}}}{\text{minimize}} & \int\limits_{\omega\in\mathcal{P}} \frac{\left[\sin(K\omega)+\mathbf{s}(\omega)\cdot\widetilde{\mathbf{v}}\right]^2\mathrm{d}\omega}{\left[\sin(K\omega)+\mathbf{s}(\omega)\cdot\widetilde{\mathbf{v}}\right]^2+v_1^2\left[\cos(K\omega)+\mathbf{c}(\omega)\cdot\mathbf{u}\right]^2} \\ \text{subject to:} & \begin{bmatrix} \boldsymbol{\gamma}_L - \boldsymbol{\eta}_L\cdot v_1 \\ \boldsymbol{\gamma}_R - \boldsymbol{\eta}_R\cdot v_1 \end{bmatrix} \leq \begin{bmatrix} \widetilde{\boldsymbol{\Phi}}_L \\ \widetilde{\boldsymbol{\Phi}}_R \end{bmatrix}\widetilde{\mathbf{v}} \leq \begin{bmatrix} \boldsymbol{\gamma}_L \\ \boldsymbol{\gamma}_R \end{bmatrix} \end{array}, \tag{49}$$

note Eqs. (16), (17), (43) and (32), where

$$\mathbf{s}\left(\omega\right) = \left[\sin\omega \quad \sin\left(2\omega\right) \quad \ldots \quad \sin\left(\left(K-1\right)\omega\right)\right]. \tag{50}$$

Now, obtained optimization problem can be efficiently solved iteratively using the Steiglitz-McBride approach [21, 17]. In this way, lower computational complexity is achieved compared to the approach in [23] that utilize the PSO algorithm. Previous optimization problem characterizes the design method referred to as *Method F-A*.

4) Method in [27] utilizes notch and both left- and right-hand cutoff frequencies as design constraints. However, as number of linear equality constraints derived from design constraints equals $3K$, while number of unknown coefficients equals $2K$, variable elimination is first performed to ensure that notch

frequencies' specifications are satisfied. Then, remaining overdetermined system of linear equations is solved in the least-square sense.

Overdetermined system from [27] can be obtained by equating the left-hand sides of Eqs. (26) and (27) to zero, followed by multiplication by $(1 - p_{2K})$ and substitution of Eqs. (43) and (32),

$$\begin{aligned} (\boldsymbol{\gamma}_L + \boldsymbol{\eta}_L)\, p_{2K} + \widetilde{\boldsymbol{\Phi}}_L\, (1 - p_{2K})\, \widetilde{\mathbf{v}} &= \boldsymbol{\gamma}_L - \boldsymbol{\eta}_L, \\ (\boldsymbol{\gamma}_R + \boldsymbol{\eta}_R)\, p_{2K} + \widetilde{\boldsymbol{\Phi}}_R\, (1 - p_{2K})\, \widetilde{\mathbf{v}} &= \boldsymbol{\gamma}_R - \boldsymbol{\eta}_R, \end{aligned} \tag{51}$$

hence, the least-square solution reads

$$\begin{bmatrix} p_{2K} \\ (1 - p_{2K})\, \widetilde{\mathbf{v}} \end{bmatrix} = \begin{bmatrix} \boldsymbol{\gamma}_L + \boldsymbol{\eta}_L & \widetilde{\boldsymbol{\Phi}}_L \\ \boldsymbol{\gamma}_R + \boldsymbol{\eta}_R & \widetilde{\boldsymbol{\Phi}}_R \end{bmatrix}^{\dagger} \cdot \begin{bmatrix} \boldsymbol{\gamma}_L - \boldsymbol{\eta}_L \\ \boldsymbol{\gamma}_R - \boldsymbol{\eta}_R \end{bmatrix}, \tag{52}$$

where † denotes Moore-Penrose inverse.

Previous equation defines the design method referred to as *Method G*.

Minimum-order allpass-based IIR multi-notch filters designed using proposed and existing methods are compared in terms of maximum pole radius, $\rho_{\max}$, and the area under the passbands squared magnitude response, A_p. Three sets of IIR multi-notch filter specifications are considered:

1. $\omega_{n,1} = 0.3\pi$, $\omega_{n,2} = 0.5\pi$, $\Delta\omega_1 = \Delta\omega_2 = 0.1\pi$, $a = 2.2$ dB
2. $\omega_{n,1} = 0.2\pi$, $\omega_{n,2} = 0.4\pi$, $\omega_{n,3} = 0.7\pi$, $\Delta\omega_1 = \Delta\omega_2 = \Delta\omega_3 = 0.1\pi$, $a = 2$ dB
3. $\omega_{n,1} = 0.1\pi$, $\omega_{n,2} = 0.2\pi$, $\omega_{n,3} = 0.4\pi$, $\omega_{n,3} = 0.8\pi$, $\Delta\omega_1 = \Delta\omega_2 = 0.06\pi$, $\Delta\omega_3 = \Delta\omega_4 = 0.08\pi$, $a = 1.75$ dB

$\rho_{\max}$, $\sqrt[4]{p_{2K}}$ and A_p of IIR multi-notch filters obtained using all discussed methods, except *Method F-A*, for all three specifications sets, are given in Tab. 1. Passbands magnitude responses of IIR multi-notch filters designed using *Methods A, B* and *D* for the first specifications set, and *Methods C-M* and *F-APNF* for the third specifications set are given in Figs. 1 and 2, respectively. As geometric means of pole radii obtained by utilization of *Methods D* and *E* are less than the values obtained when *Method A* utilized, note Tab. 1, specifications regarding the maximum attenuation value in passbands are not satisfied

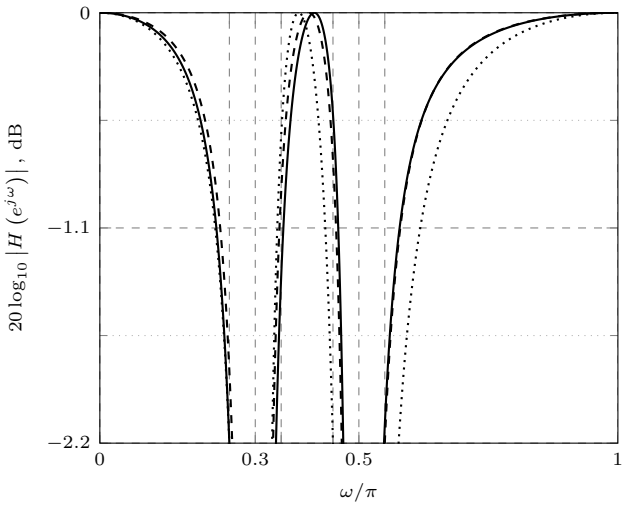

Figure 1: First specifications set: dashed, solid and dotted lines correspond to passbands magnitude responses of filters obtained by *Methods A, B* and *D*, respectively.

when *Methods D* and *E* are utilized for all three specifications sets. For the same reason, specifications are not met when *Method G* utilized for the first two specifications sets, while it also shows that passbands magnitude response specifications are not satisfied for the third specifications set. This can be also concluded from Fig. 1 for the filter obtained using *Method D*.

From Tab. 1 it can be observed that for the first two specification sets, utilization of the *Method B* results in the highest A_p ($\sqrt[4]{p_{2K}}$), while for the third specifications set *Method F-LMPN* provides the highest A_p ($\sqrt[4]{p_{2K}}$). Regarding the maximum pole radius, $\rho_{\max}$, the second best design methods (as utilization of *Method C-M* yields the lowest $\rho_{\max}$) are *Methods C-L, F-LMPN* and *A* for the first, second and third specifications sets, respectively. For considered design methods, it can be also concluded that higher geometric mean of pole radii is not necessarily followed by higher A_p. Furthermore, unless maximum pole radius is required to be minimized, performances of all methods are specifications-specific. For example, *Method B* outperforms *Method F-APNF* both in terms of stability margin ($\rho_{\max}$) and A_p for the second specifications set, while opposite is true for the third specifications set.

Table 1: Maximum pole radii, geometric mean of the pole radii and the areas under the passbands magnitude responses of IIR multi-notch filters obtained using all discussed methods except *Method F-A*.

	1st specs. set			2nd specs. set			3rd specs. set		
Method	$\rho_{\max}$	$\sqrt[4]{p_{2K}}$	A_p	$\rho_{\max}$	$\sqrt[4]{p_{2K}}$	A_p	$\rho_{\max}$	$\sqrt[4]{p_{2K}}$	A_p
A	0.9020	0.8928	1.9912	0.8974	0.8397	1.6469	0.9440	0.8614	1.7586
B	0.9065	0.9015	2.0523	0.9213	0.8684	1.7764	0.9808	0.8851	1.8345
C-L	0.8985	0.8985	2.0322	0.9056	0.8497	1.6930	0.9839	0.8912	1.8390
C-R	0.9053	0.8941	1.9992	0.8972	0.8419	1.6566	0.9455	0.8619	1.7605
C-LR	0.9020	0.8928	1.9912	0.8971	0.8407	1.6513	0.9802	0.8866	1.8392
C-M	0.8984	0.8984	2.0319	0.8956	0.8476	1.6847	0.9404	0.8640	1.7744
D	0.8950	0.8676	1.8235	0.8924	0.8048	1.4860	0.9377	0.8212	1.5594
E	0.9098	0.8813	1.9020	0.8990	0.8299	1.5918	0.9492	0.8579	1.7310
F-PANF	0.9050	0.9009	2.0486	0.9199	0.8666	1.7690	0.9578	0.8826	1.8615
F-APNF	0.8989	0.8977	2.0268	0.9313	0.8676	1.7671	0.9638	0.8930	1.9044
F-LMPN	0.8989	0.8977	2.0268	0.8961	0.8455	1.6746	0.9496	0.8963	1.9330
G	0.8876	0.8846	1.9392	0.8886	0.8328	1.6156	0.9805	0.8855	1.8331

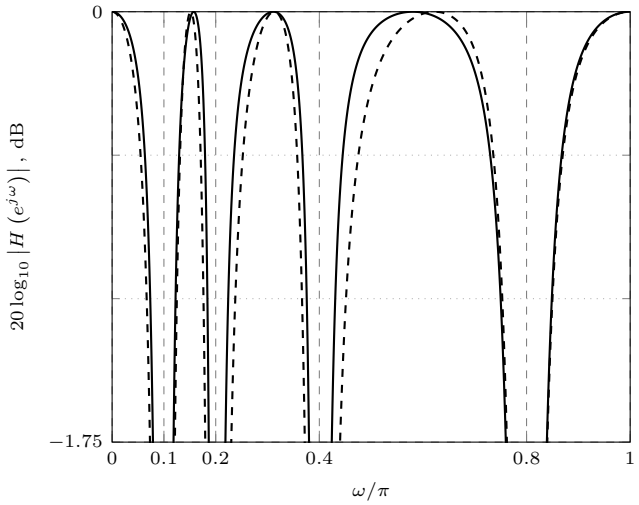

Figure 2: Third specifications set: dashed and solid lines correspond to passbands magnitude responses of filters obtained by *Methods C-M* and *F-APNF*, respectively.

Geometric means of pole radii that correspond to filters designed using *Methods A, B, C-L, C-R, C-LR, C-M, F-PANF, F-APNF* and *F-LMPN* are used

Table 2: *Method F-A*: Maximum pole radii and the areas under the passbands magnitude responses of IIR multi-notch filters for all three specifications sets and various values of the geometric mean of the pole radii. *Method** column indicates a method which utilization results in the same geometric mean of pole radii.

	1st specs. set			2nd specs. set			3rd specs. set		
*Method**	$\sqrt[4]{p_{2K}}$	$\rho_{\max}$	A_p	$\sqrt[4]{p_{2K}}$	$\rho_{\max}$	A_p	$\sqrt[4]{p_{2K}}$	$\rho_{\max}$	A_p
A	0.8928	0.9020	1.9912	0.8397	0.8974	1.6469	0.8614	0.9440	1.7586
B	0.9015	0.9032	2.0527	0.8684	0.9105	1.7847	0.8851	0.9511	1.8852
C-L	0.8985	0.9002	2.0320	0.8497	0.8973	1.6946	0.8912	0.9539	1.9166
C-R	0.8941	0.9012	2.0013	0.8419	0.8969	1.6572	0.8619	0.9434	1.7617
C-LR	0.8928	0.9020	1.9912	0.8407	0.8972	1.6515	0.8866	0.9518	1.8932
C-M	0.8984	0.9002	2.0317	0.8476	0.8959	1.6847	0.8640	0.9413	1.7744
F-PANF	0.9009	0.9026	2.0488	0.8666	0.9092	1.7758	0.8826	0.9500	1.8723
F-APNF	0.8977	0.8995	2.0268	0.8676	0.9099	1.7809	0.8930	0.9547	1.9259
F-LMPN	0.8977	0.8995	2.0268	0.8455	0.8961	1.6746	0.8963	0.9561	1.9428

as a starting point for *Method F-A*, for all three specifications sets. $\rho_{\max}$, $\sqrt[4]{p_{2K}}$ and A_p of obtained filters are provided in Tab. 2. As in the first example, the highest values for the A_p are obtained when geometric means of the pole radii equal the values obtained by the utilization of the *Method B* for the first two specifications sets, and *Method F-LMPN* for the third specifications set. However, as opposed to the previously discussed design methods, higher geometric mean of pole radii is followed by higher A_p, for all three considered specifications sets, note Tab. 2. From Tabs. 1 and 2 it can be also concluded that if minimum value of the geometric mean of pole radii is specified in *Method F-A*, obtained $\rho_{\max}$ and A_p are the same as if *Method A* used, ie. the same transfer functions are obtained. In other words, it seems that there are no two multi-notch filters with minimum value of geometric mean of pole radii.

5. Conclusion

In this paper, comprehensive literature review of the minimum order IIR multi-notch filter design methods is first performed, and several allpass-based design methods are derived such that various cost functions are minimized.

Additionally, it is shown that IIR multi-notch filter transfer functions derived using some of the existing design methods can be alternatively derived using conclusions drawn and notations introduced in the paper, and as for design methods from [23], a lower computational complexity counterpart methods are obtained.

Results of comparison with the existing design methods show that proposed *Method C-M* outperforms existing methods in terms of stability margin. Therefore, its utilization is preferred in all applications where IIR multi-notch filters are realized using finite wordlength. As of *Method B*, its utilization can result in transfer functions having the highest area under the passbands magnitude response as compared to transfer functions obtained by means of all methods except *Method F-A* (since this method requires the geometric mean of pole radii to be specified). Regarding the utilization of the *Method F-A*, higher specified geometric mean of pole radii is followed by the higher area under the passbands magnitude response.

References

[1] R. K. Mahendran, P. Velusamy, P. Pandian, An efficient priority-based convolutional auto-encoder approach for electrocardiogram signal compression in Internet of Things based healthcare system, Transactions on Emerging Telecommunications Technologies 32 (1) (2021) e4115.

[2] A. Appathurai, J. J. Carol, C. Raja, S. Kumar, A. V. Daniel, A. J. G. Malar, A. L. Fred, S. Krishnamoorthy, A study on ECG signal characterization and practical implementation of some ECG characterization techniques, Measurement 147 (2019) 106384.

[3] J. Piskorowski, Time-efficient removal of power-line noise from EMG signals using IIR notch filters with non-zero initial conditions, Biocybernetics and Biomedical Engineering 33 (3) (2013) 171–178.

[4] H. Zhao, Y. Hu, H. Sun, W. Feng, A BDS Interference Suppression Technique Based on Linear Phase Adaptive IIR Notch Filters, Sensors 18 (5) (2018) 1515.

[5] X.-L. Wang, Y.-J. Ge, J.-J. Zhang, Q.-J. Song, Discussion on the -3 dB rejection bandwidth of IIR notch filters, in: Signal Processing, 2002 6th International Conference on, Vol. 1, IEEE, 2002, pp. 151–154.

[6] J. Piskorowski, Digital Q-Varying Notch IIR Filter With Transient Suppression, IEEE Transactions on Instrumentation and Measurement 59 (4) (2010) 866–872.

[7] L. Tan, J. Jiang, L. Wang, Pole-radius-varying IIR notch filter with transient suppression, IEEE Transactions on Instrumentation and Measurement 61 (6) (2012) 1684–1691.

[8] S. Nikolić, G. Stančić, Design of IIR Notch Filter with Approximately Linear Phase, Circuits, Systems, and Signal Processing 31 (6) (2012) 2119–2131. doi:10.1007/s00034-012-9426-x.

[9] G. Stančić, S. Nikolić, Digital linear phase notch filter design based on IIR all-pass filter application, Digital Signal Processing: A Review Journal 23 (3) (2013) 1065–1069. doi:10.1016/j.dsp.2013.01.006.

[10] Y. Jiang, C. Shen, J. Dai, A unified approach to the design of IIR and FIR notch filters, in: 2016 IEEE International Conference on Acoustics, Speech and Signal Processing (ICASSP), 2016, pp. 4791–4795. doi:10.1109/ICASSP.2016.7472587.

[11] I. Krstić, S. Nikolić, G. Stančić, P. Lekić, Design of IIR multiple-notch filters with symmetric magnitude responses about notch frequencies, Circuits, Systems, and Signal Processing 37 (12) (2018) 5616–5636. doi:10.1007/s00034-018-0841-5.

[12] S. Nikolić, I. Krstić, G. Stančić, Noniterative design of IIR multiple-notch filters with improved passband magnitude response, International Journal

of Circuit Theory and Applications 46 (12) (2018) 2561–2567. doi:10.1002/cta.2525.

[13] P. A. Regalia, S. K. Mitra, P. Vaidyanathan, The digital all-pass filter: A versatile signal processing building block, Proceedings of the IEEE 76 (1) (1988) 19–37.

[14] S. Pei, W. Lu, B. Guo, Pole–Zero Assignment of All-Pass-Based Notch Filters, IEEE Transactions on Circuits and Systems II: Express Briefs 64 (4) (2017) 477–481.

[15] A. Thamrongmas, C. Charoenlarpnopparut, All-pass based IIR multiple notch filter design using Gröbner Basis, in: Multidimensional (nD) Systems (nDs), 2011 7th International Workshop on, IEEE, 2011, pp. 1–6.

[16] Q. Wang, D. Kundur, A generalized design framework for IIR digital multiple notch filters, EURASIP Journal on Advances in Signal Processing 2015 (1) (2015) 26.

[17] C.-C. Tseng, S.-C. Pei, Stable IIR notch filter design with optimal pole placement, IEEE Transactions on Signal processing 49 (11) (2001) 2673–2681.

[18] Q. Wang, J. Song, H. Yuan, Digital multiple notch filter design based on genetic algorithm, in: Instrumentation and Measurement, Computer, Communication and Control (IMCCC), 2014 Fourth International Conference on, IEEE, 2014, pp. 180–183.

[19] S. Yimman, S. Praesomboon, P. Soonthuk, K. Dejhan, IIR multiple notch filters design with optimum pole position, in: 2006 International Symposium on Communications and Information Technologies, ISCIT, 2006. doi:10.1109/ISCIT.2006.340048.

[20] Q. Wang, D. Kundur, H. Yuan, Y. Liu, J. Lu, Z. Ma, Noise suppression of corona current measurement from HVdc transmission lines, IEEE transactions on instrumentation and measurement 65 (2) (2015) 264–275.

[21] K. Steiglitz, L. McBride, A technique for the identification of linear systems, IEEE Transactions on Automatic Control 10 (4) (1965) 461–464.

[22] Y. Joshi, S. D. Roy, Design of IIR multiple notch filters, International Journal of Circuit Theory and Applications 26 (5) (1998) 499–507.

[23] C. Duarte, K. E. Barner, K. Goossen, Design of IIR multi-notch filters based on polynomially-represented squared frequency response, IEEE Transactions on Signal Processing 64 (10) (2016) 2613–2623.

[24] S. C. Pei, C. C. Tseng, IIR multiple notch filter design based on allpass filter, in: TENCON '96. Proceedings., 1996 IEEE TENCON. Digital Signal Processing Applications, Vol. 1, 1996, pp. 267–272 vol.1. doi:10.1109/TENCON.1996.608814.

[25] S. C. Pei, C. C. Tseng, IIR multiple notch filter design based on allpass filter, IEEE Transactions on Circuits and Systems II: Analog and Digital Signal Processing 44 (2) (1997) 133–136. doi:10.1109/82.554450.

[26] Q. Wang, X. Gu, J. Lin, Adaptive notch filter design under multiple identical bandwidths, AEU-International Journal of Electronics and Communications 82 (2017) 202–210.

[27] I. Krstić, The least-square design of minimum-order allpass-based infinite impulse response multi-notch filters, International Journal of Circuit Theory and Applications 49 (8) (2021) 2643–2650. doi:10.1002/cta.3100.

[28] M. C. Lang, Weighted least squares IIR filter design with arbitrary magnitude and phase responses and specified stability margin, in: Advances in Digital Filtering and Signal Processing, 1998 IEEE Symposium on, IEEE, 1998, pp. 82–86.